FULL PAPER

Synthesis, Crystal Structure, and Magnetic Property of New Trispin Ln(III)-Nitronyl Nitroxide Complexes

by **Zhe Fan**[a]), **Yi-Fang Hou**[a]), **Shu-Ping Wang***[a]), **Shu-Tao Yang**[a]), **Jian-Jun Zhang**[b]), **Shi-Kao Shi**[a]), and **Li-Na Geng**[a])

[a]) College of Chemistry & Material Science, Hebei Normal University, Shijiazhuang 050024, P. R. China (phone: +86 31180787400; e-mail: pingwsh@mail.hebtu.edu.cn)

[b]) Experimental Center, Hebei Normal University, Shijiazhuang 050024, P. R. China

Four Ln(III) complexes based on a new nitronyl nitroxide radical have been synthesized and structurally characterized: {Ln(hfac)$_3$[NITPh(MeO)$_2$]$_2$} (Ln = Eu(**1**), Gd(**2**), Tb(**3**), Dy(**4**); NITPh(MeO)$_2$ = 2-(3′,4′-dimethoxyphenyl)-4,4,5,5-tetramethylimidazoline-1-oxyl-3-oxide; hfac = hexafluoroacetylacetonate). The single-crystal X-ray diffraction analysis shows that these complexes have similar mononuclear trispin structures, in which central Ln(III) ion is eight-coordinated by two O-atoms from two nitroxide groups and six O-atoms from three hfac anions. The variable temperature magnetic susceptibility study reveals that there exist ferromagnetic interactions between Gd(III) and the radicals, and antiferromagnetic interactions between two radicals ($J_{Gd\text{-}Rad}$ = 3.40 cm^{-1}, $J_{Rad\text{-}Rad}$ = −9.99 cm^{-1}) in complex **2**. Meanwhile, antiferromagnetic interactions are estimated between Eu(III) (or Dy(III)) and radicals in complexes **1** and **4**, and ferromagnetic interaction between Tb(III) and radicals in complex **3**, respectively.

Keywords: Nitronyl nitroxide, Rare earth metal complexes, Structure elucidation, Magnetic properties.

Introduction

The design and synthesis of novel molecular-based magnetic materials, which combine paramagnetic metal ions with organic radicals as multispin systems, have attracted great attention over the past decades [1 – 4], due to their potential applications in high-density information storage, quantum computation, and spintronic devices [5 – 7]. Among these researches, the interest toward lanthanide-based systems is steadily increasing [8]. Otherwise, based on the unquenched orbital angular momentum and strong spin–orbit coupling of Ln(III) ions, it is difficult to carry out a strictly quantitative treatment of magnetic interactions for most of these lanthanides complexes, except for the isotropic Gd(III) [9 – 13]. It is a great challenge for magnetochemists to study the nature of magnetic interactions between Ln(III) ions and organic radicals. Therefore, obtaining more lanthanide complexes and studying their magnetic behaviors systematically is very meaningful.

Since the discovery of first single chain magnet [Co(hfac)$_2$(NITPhMeO)] by *Gatteschi* [14], lanthanide-radical approach has become an effective method to obtain the slow-relaxing molecular magnets, such as single chain magnets (SCMs) [15 – 19], single molecule magnets (SMMs) [20 – 30], and other particular magnetic systems [31 – 35]. In these designing strategies, Tb(III) and Dy(III) are selected as preferred central ions due to their large magnetic anisotropy. The reported SCMs mainly involve the 1D-Ln(III)-nitronyl nitroxide radicals (NITR) complexes with R = PhOPh-, MeSPh-, thien-2-yl, and 3-bromothien-2-yl, respectively. The SMMs include the dinuclear or mononuclear Ln(III)-NITR, Ln(III)-IMR, and Ln(III)-biradical complexes with R = -4Py, -3Py, -2Py, -5-Br-3Py, -PhOEt, Ph, thiazol-2-yl, -2Py-3-COOH, -PhOH, *etc*. These works demonstrate that the substituents of NITR play a crucial role in modulating the molecule structure, crystalline structure, and the ultimate magnetic behaviors for these coordination systems. To explore and study more 2p-4f magnetic systems, we synthesized a new nitronyl nitroxide radical NITPh(MeO)$_2$, with two MeO groups on the Ph ring of R substituent in NITR. Furthermore, we obtained four Ln(III)-radical mononuclear trispin complexes. Their crystal structures and magnetic properties were studied. Although no slow-relaxing molecular magnet is found, the study about the magnetic property is meaningful for the basic theoretical study of lanthanide-radical complexes.

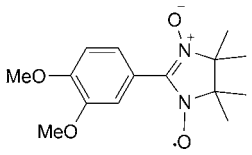

NITPh(MeO)$_2$

 DOI: 10.1002/hlca.201600152

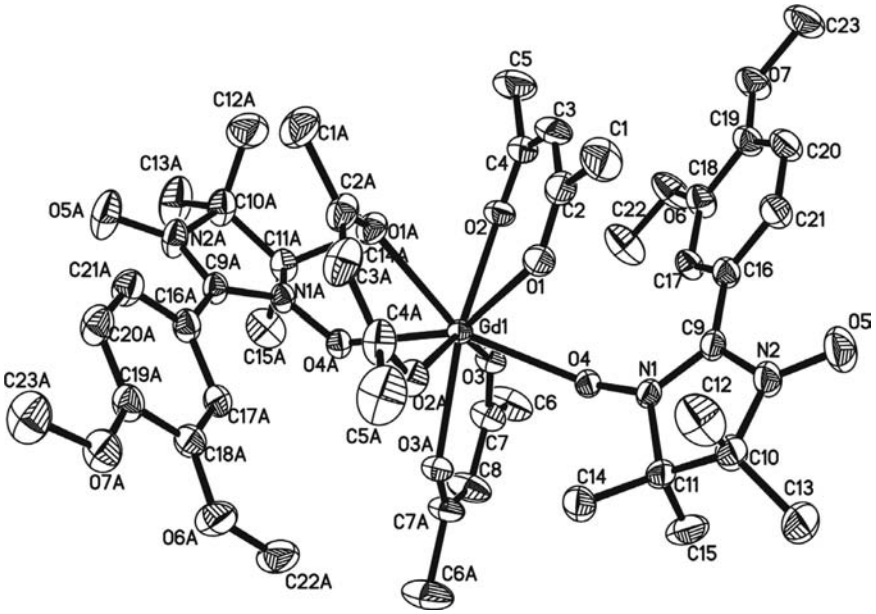

Fig. 1. Molecular structure of $Gd(hfac)_3[NITPh(MeO)_2]_2$ (**2**) with the thermal ellipsoids at 30% probability level. All H- and F-atoms are omitted for clarity.

Results and Discussion

Crystal Structures

Single-crystal X-ray diffraction analyses reveal that the molecular structures of complexes **1** – **4** are isostructural, and belong to the monoclinic system with space group *C*2/*c*. They all show mononuclear trispin (radical-Ln(III)-radical) structures, of which two nitronyl nitroxide radicals act as monodentate ligands. Therefore, only the molecular structure of complex **2** is shown in *Fig. 1* as an example, the other complexes are shown in Fig. S1 – S3 in the Supporting Information (SI). In complex **2**, the Gd (III) ion is eight-coordinated, of which six O-atoms from three bidentate hfac anions with the Gd–O(hfac) bond lengths in the range 2.348(2) – 2.424(2) Å, and two O-atoms from two nitroxide groups with the Gd–O(rad) bond lengths of 2.344(2) Å, respectively. The coordination polyhedron around Gd(III) ion may be represented as a distorted dodecahedron with triangular faces (*Fig. 2*) [36]. The coordinated N(1)–O(4) bond lengths of the nitronyl nitroxide radicals is 1.310(3) Å, which are a little longer than the uncoordinated N(2)–O(5), and the bond angle of O(4)–Gd–O(4A) is 143.3(2)°. These bond lengths are comparable to those of the $Ln(hfac)_3$-nitronyl nitroxide complexes in literature [13][37][38]. The packing diagram for complex **2** is shown in *Fig. 3*, and the perspective drawing seem like wave lines. There is no H-bonding or π–π stacking interaction between the molecules. The shortest intermolecular distance of uncoordinated O-atoms between the N–O groups is 4.735 Å, and the nearest distance of Gd(III)···Gd(III) between the adjacent molecules is 11.722 Å. For other complexes, because of the lanthanide contraction phenomena, different central ions result in different crystal parameters; bond lengths and bond angles vary a little.

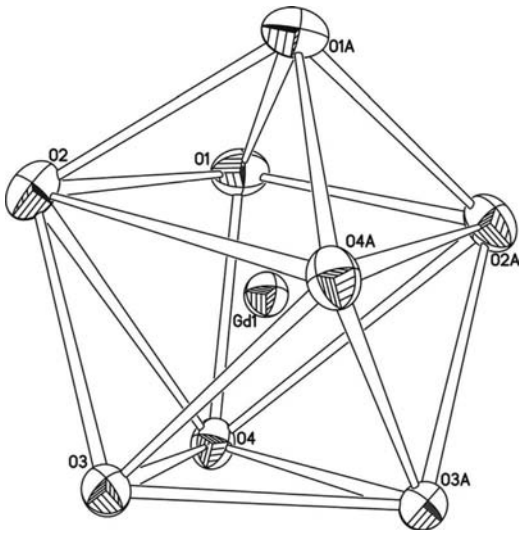

Fig. 2. The coordination geometry of Gd(III) ion in **2**.

Magnetic Properties

Magnetic measurements were performed on polycrystalline samples of **1** – **4**. The phase purity of the bulk samples was confirmed by XRD analyses as shown in Fig. S4 – S7 (SI).

Static Magnetic Property of Complex **1**

The temperature dependence of the $\chi_M T$ product for the Eu(**1**) is shown in *Fig. 4*. The $\chi_M T$ value is 2.38 cm^3 K/mol

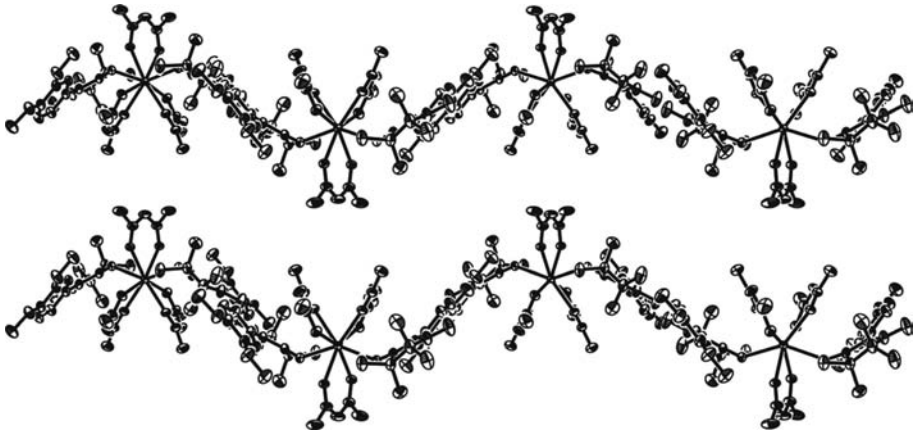

Fig. 3. Packing diagram of **2**, the H- and F-atoms are omitted for clarity.

at room temperature, slightly higher than the theoretical sum of a Eu(III) ion (1.5 cm^3 K/mol calculated by *Van Vleck* allowing for population of the excited state with higher values of J at 293 K [39] and two organic radicals (0.75 cm^3 K/mol). Upon cooling, the $\chi_M T$ value decreases, only the nonmagnetic ground state $^7F_0$ of Eu(III) is populated, there is no *Stark* sublevel from the ligand field. Thus, χ_{Eu} can be given as a function of the spin–orbit coupling parameter (λ) in *Eqn. 1* [22].

The magnetic susceptibility of radical NITPh(MeO)$_2$

$$\chi_{Eu} = \frac{N\beta^2}{3kTx}\left[\frac{24 + (13.5x - 1.5)e^{-x} + (67.5x - 2.5)e^{-3x} + (189x - 3.5)e^{-6x} + (405x - 4.5)e^{-10x} + (742.5x - 5.5)e^{-15x} + (1228.5x - 6.5)e^{-21x}}{1 + 3e^{-x} + 5e^{-3x} + 7e^{-6x} + 9e^{-10x} + 11e^{-15x} + 13e^{-21x}}\right]; x = \frac{\lambda}{kT} \quad (1)$$

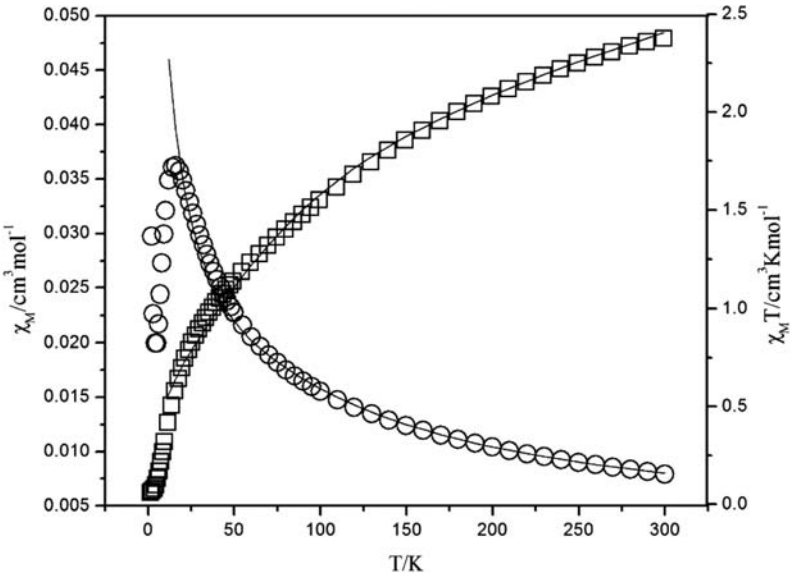

Fig. 4. Temperature dependence of χ_M (○) and $\chi_M T$ (□) *vs.* T for Eu(**1**). The solid line corresponds to the best theoretical fit.

and nearly to zero at 2 K. The ground state $^7F_0$ of Eu(III) is nonmagnetic, and the first excited state $^7F_1$ of Eu(III) is at *ca.* 350 cm^{-1}, which is sufficiently low in energy to be thermally populated at room temperature [22]. The decrease in $\chi_M T$ values on lowering the temperature attributes to the thermal depopulation of the excited levels. If (χ_{Rad}) may be expressed as in *Eqn. 2*. Based on the structural units of complex **1**, there is no available theoretical expression to determine the magnetic susceptibility of such system with large magnetic anisotropy. Its magnetic susceptibility is approximately treated as a sum of the contributions of one Eu(III) ion and two radicals

($\chi_{total} = 2\chi_{Rad} + \chi_{EU}$), and the molecular field approximation (zJ') is introduced to roughly take into account the magnetic interaction parameters between the paramagnetic species as *Eqn. 3*.

$$\chi_{Rad} = \frac{Ng_R^2\beta^2}{3kT}\frac{1}{2}\left(\frac{1}{2}+1\right) \quad (g_R = 2) \tag{2}$$

$$\chi_{MF} = \frac{\chi_{total}}{1-(2zJ'/Ng^2\beta^2)\chi_{total}} \tag{3}$$

The best fit gives $g = 1.97$, $\lambda = 175\ cm^{-1}$, $zJ' = -4.16\ cm^{-1}$ in the range of 12 – 300 K. The negative zJ' suggests antiferromagnetic interaction between the paramagnetic species in the mononuclear system. Note that the ground state of Eu(III) is nonmagnetic, thus the low-temperature magnetic behavior for complex **1** is governed by the interaction between two paramagnetic radicals. The rapid decrease in $\chi_M T$ and χ_M below 12 K can be attributed to antiferromagnetic interactions between two nitronyl nitroxide units *via* diamagnetic Eu (III). The interaction parameter ($-4.16\ cm^{-1}$) is comparable with the values found previously for the compounds involving Eu(III) (-1.2 and $-3.19\ cm^{-1}$) [22][40].

Static Magnetic Property of Complex **2**

For Gd(**2**), its magnetic behavior is shown in *Fig. 5*. The $\chi_M T$ value is 8.86 cm^3 K/mol at room temperature, which is close to the expected value of 8.63 cm^3 K/mol for an uncoupled Gd^{III} ion ($^8S_{7/2}$, g = 2) plus two radicals. As the temperature is decreased, the $\chi_M T$ value increase steadily and reach a maximum of 11.08 cm^3 K/mol at 3 K, then decreases to 11.00 cm^3 K/mol at 2 K.

Gd(III) is easier to be studied than other lanthanide ions, due to half-filled $4f^7$ electron configuration. There are two kinds of magnetic interactions in the trispin system: *i*) the interactions between Gd(III) and radical (J_1), and *ii*) intramolecular interactions between two radicals (J_2). To evaluate the exchange coupling constants in such a magnetic system, considering Gd(III) with an $^8S_{7/2}$ ground state, its magnetic interaction with the radical can be well described by isotropic exchange interaction. The magnetic analysis is carried out using the spin *Hamiltonian* (*Eqn. 4*). Taking the low-temperature molecular field approximation (zJ') into account, the magnetic data is fitted by the following theoretical *Eqns. 5* and *6* [41].

$$\hat{H} = -2J_1\left(\hat{S}_{Gd}\cdot\hat{S}_{R1} + \hat{S}_{Gd}\hat{S}_{R2}\right) - 2J_2\cdot\hat{S}_{R1}\cdot\hat{S}_{R2} \tag{4}$$

$$\chi_{Gd} = \frac{Ng_2^2\beta^2}{4kT}\left[\frac{165+84\exp(\frac{-9J_1}{kT})+84\exp(\frac{-7J_1-2J_2}{kT})+35\exp(\frac{-16J_1}{kT})}{5+4\exp(\frac{-9J_1}{kT})+4\exp(\frac{-7J_1-2J_2}{kT})+3\exp(\frac{-16J_1}{kT})}\right] \tag{5}$$

$$\chi_2 = \frac{\chi_{Gd}}{1-(2zJ'/Ng^2\beta^2)\chi_{Gd}} \tag{6}$$

The best fitting parameters are $g = 2.01$, $J_1 = 3.40\ cm^{-1}$, $J_2 = -9.99\ cm^{-1}$, and $zJ' = -1.0 \times 10^{-2}\ cm^{-1}$ with the agreement factor $R = 1.47 \times 10^{-5}$. The positive J_1 value indicates that there is weak ferromagnetic interaction between Gd(III) ion and the NITPh $(MeO)_2$ radicals, and the negative J_2 shows the antiferromagnetic interaction between two radicals. The Gd-radical ferromagnetic interaction can be explained based on the electron transfer of the unpaired electron in radical into the empty 5d orbitals of Gd(III) ion, resulting in the parallel alignment of 4f and 5d electrons according the *Hund* rule [42].

The field dependence of magnetization for complex **2** was measured at 2 K in the range of 0 – 70 kOe, and the *M–H* plot is shown in SI (Fig. S8). The experimental magnetization is compared to the theoretical magnetization

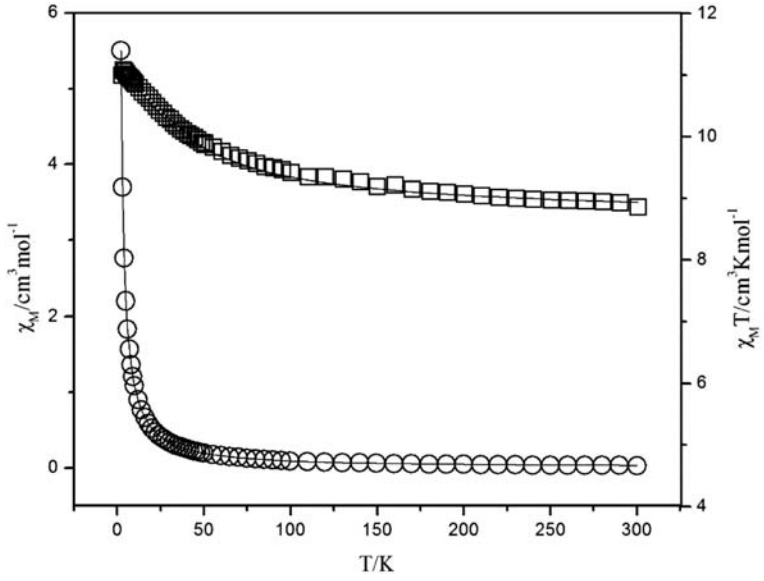

Fig. 5. Temperature dependence of χ_M (○) and $\chi_M T$ (□) *vs. T* for Gd(**2**). The solid line corresponds to the best theoretical fit.

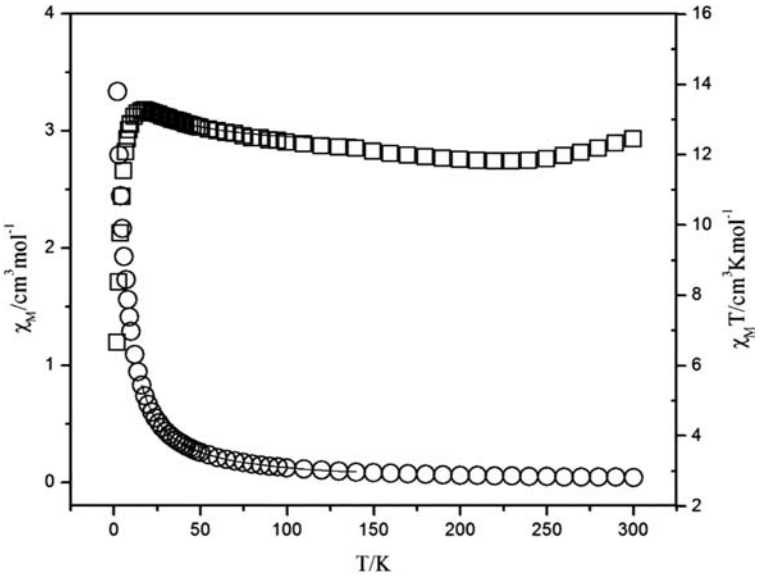

Fig. 6. Temperature dependence of χ_M (○) and $\chi_M T$ (□) *vs. T* for Tb(**3**). The solid line corresponds to the best theoretical fit.

given by the *Brillouin* function for a S = 9/2 total spin and to the sum of isolated Gd(III) and nitronyl nitroxides (S_{Gd} = 7/2 + 2 × S_{rad} = 1/2). For any value of the field, the experimental magnetization is larger than that of the noncorrelated spin system but very close to the value expected for the S = 9/2 ferromagnetic state. This is the further evidence of ferromagnetic interaction between Gd (III) ion and the radicals.

Static Magnetic Properties of Complexes **3** *and* **4**

The temperature dependence of magnetic susceptibilities for complexes Tb(**3**) and Dy(**4**) are displayed in *Fig. 6* and *7*, respectively. The $\chi_M T$ values are 12.45 and 14.31 cm^3 K/mol at room temperature, which are slightly lower than the expected values of 12.56 and 14.92 cm^3 K/mol for an uncoupled Ln(III) ion ($^7F_6$, g = 3/2 for Tb (III); $^6H_{15/2}$, g = 4/3 for Dy(III)) plus two radicals. For Tb (**3**) upon cooling, the $\chi_M T$ value decreases slightly above 190 K, and then increases smoothly and reaches a maximum of 13.26 cm^3 K/mol at 18 K, then decreases sharply to a minimum of 6.67 cm^3 K/mol at 2 K. For complex Dy (**4**), the $\chi_M T$ value decreases gradually and reaches a minimum of 7.70 cm^3 K/mol at 2 K.

It is known that the coupled systems including at least one ion with an orbital momentum are not amenable to quantitative analysis. The obvious feature of complexes Tb(**3**) and Dy(**4**) is the intrinsic magnetic anisotropy of Ln(III) ion. With the strong spin–orbit coupling and large magnetic anisotropy of Ln(III), it is difficult to carry out a strictly theoretical model to analyze the magnetic behavior of Ln(III) complexes. To obtain a rough quantitative estimate of the magnetic interaction parameters between paramagnetic species, we refer to the similar Ln(III)-radical complexes in the literature [38][41]. The magnetic susceptibilities of Tb(**3**) and Dy(**4**) can be roughly calculated as a sum of a Ln(III) and two uncoupled NITPh(MeO)$_2$ radicals (*Eqn. 7*). The Ln(III) ion may exhibit a splitting of the M_J energy levels ($\hat{H} = \Delta \hat{J}_z^2$) in a axial crystal field. Thus χ_{Tb} and χ_{Dy} can be described by the expression (*Eqns. 8* and *9*) [41].

$$\chi = 2\chi_R + \chi_{Ln} = \frac{Ng_R^2\beta^2}{2kT} + \chi_{Ln} \tag{7}$$

$$\chi_{Tb} = \frac{2Ng_3^2\beta^2}{kT}\left[\frac{36\exp(\frac{-36\Delta_3}{kT}) + 25\exp(\frac{-25\Delta_3}{kT}) + 16\exp(\frac{-16\Delta_3}{kT}) + 9\exp(\frac{-9\Delta_3}{kT}) + 4\exp(\frac{-4\Delta_3}{kT}) + \exp(\frac{-\Delta_3}{kT})}{2\exp(\frac{-36\Delta_3}{kT}) + 2\exp(\frac{-25\Delta_3}{kT}) + 2\exp(\frac{-16\Delta_3}{kT}) + 2\exp(\frac{-9\Delta_3}{kT}) + 2\exp(\frac{-4\Delta_3}{kT}) + 2\exp(\frac{-\Delta_3}{kT}) + 1}\right]; g_3 = 3/2 \tag{8}$$

$$\chi_{Dy} = \frac{Ng_4^2\beta^2}{4kT}\left[\frac{\begin{array}{c}225\exp(\frac{-225\Delta_4}{4kT}) + 169\exp(\frac{-169\Delta_4}{4kT}) + 121\exp(\frac{-121\Delta_4}{4kT}) + 81\exp(\frac{-81\Delta_4}{4kT}) \\ +49\exp(\frac{-49\Delta_4}{4kT}) + 25\exp(\frac{-25\Delta_4}{4kT}) + 9\exp(\frac{-9\Delta 4}{4kT}) + \exp(\frac{-\Delta_4}{4kT})\end{array}}{\begin{array}{c}\exp(\frac{-225\Delta_4}{4kT}) + \exp(\frac{-169\Delta_4}{4kT}) + \exp(\frac{-121\Delta_4}{4kT}) + \exp(\frac{-81\Delta_4}{4kT}) \\ + \exp(\frac{-49\Delta_4}{4kT}) + \exp(\frac{-25\Delta_4}{4kT}) + \exp(\frac{-9\Delta_4}{4kT}) + \exp(\frac{-\Delta_4}{4kT})\end{array}}\right]; g_4 = 4/3 \tag{9}$$

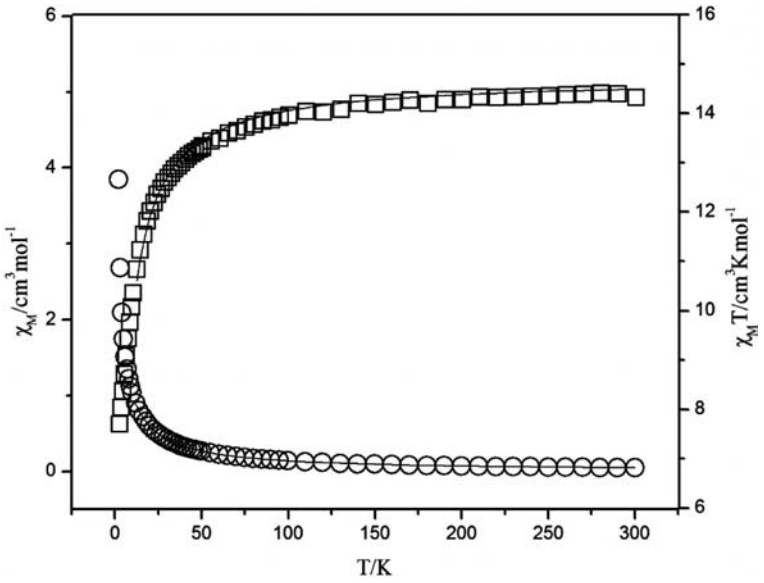

Fig. 7. Temperature dependence of χ_M (○) and $\chi_M T$ (□) *vs.* T for Dy(**4**). The solid line corresponds to the best theoretical fit.

In these expressions, Δ_3 and Δ_4 represent the zero-field-splitting parameter for Tb(III) and Dy(III), respectively. The molecular field approximation (zJ') parameter is introduced to roughly simulate the magnetic interactions between the paramagnetic species (*Eqn. 10*).

$$\chi_M = \frac{\chi}{1 - (2zJ'/Ng^2\beta^2)\chi} \tag{10}$$

The best fitting parameters for complex **3**: $g = 1.48$, $\Delta_3 = 0.43$ cm^{-1}, $zJ' = 0.21$ cm^{-1} in the range of 16 – 140 K; for complex **4**: $g = 1.32$ $\Delta_4 = -5.03 \times 10^{-3}$ cm^{-1}, $zJ' = -7.39 \times 10^{-2}$ cm^{-1} from 12 to 300 K. The positive zJ' value for Tb(**3**) indicates the weak ferromagnetic interaction between Tb(III) and radicals, and the negative zJ' value for Dy(**4**) is indicative of antiferromagnetic interaction between Dy(III) and radicals.

The field dependence of magnetization for Tb(**3**) and Dy(**4**) was determined at 2 K in the range of 0 – 70 kOe (*Fig. 8*). For Tb(**3**), the field-dependent magnetization value increases smoothly, and up to 6.63 $N\beta$ at 70 kOe, which does not reach the expected saturation values of 11 $N\beta$ (9 $N\beta$ for one Tb(III) for $J = 6$ and $g = 3/2$, plus 2 $N\beta$ for two organic radicals). Similarly for Dy(**4**), M reaches 6.63 $N\beta$ at 70 kOe, which also does not reach the saturation values of 12 $N\beta$ (10 $N\beta$ for one Dy(III) for $J = 15/2$ and $g = 4/3$, plus 2 $N\beta$ for two radicals). Similar results were reported previously [43], which can be attributed to the magnetic anisotropy and presence of low-lying excited states from Ln(III) ion.

Dynamic Magnetic Properties for **3** *and* **4**

Tb(III) and Dy(III) complexes are always appealing candidates to be SMMs or SCMs, based on their large magnetic anisotropy. Therefore, the alternating current (AC) susceptibilities were measured for Tb(**3**) and Dy(**4**) (shown in Fig. S9 and S10 in SI). Unfortunately, their imaginary component (χ'') shows a very weak signal at low temperature, and no peak appears. Thus, they do not express SMMs behavior.

For the present Ln(III)-radical magnetic systems, there are mainly two kinds of magnetic interactions, namely: *i*) Ln(III) interacting with the directly coordinated NO groups; and *ii*) Rad–Rad interaction *via* Ln (III), which may be antiferromagnetic in nature from the isostructural Gd(**2**) and other reported complexes [13]. Nevertheless, the intrinsic low overlap between 4f magnetic orbital and 2p magnetic orbital of NITR leads to the small exchange interactions observed in these complexes. The crystal field and spin–orbit effect should be dominant for their magnetic behaviors due to the strongly screened 4f orbitals by the 5s and 5p orbitals. The overall magnetic behaviors of Ln(III)-radical complexes are the comprehensive results of magnetic interactions between paramagnetic species, spin–orbit coupling, crystal field effect, and the depopulation of Ln(III) *Stark* levels. For Eu(**1**), the decrease in $\chi_M T$ value mainly attributes to the thermal depopulation of the excited levels of Eu(III) and the interactions between the paramagnetic species (Eu(III) ion and radicals) above 12 K, and the rapid decrease in χ_M and $\chi_M T$ below 12 K can be attributed to antiferromagnetic interactions between two nitronyl nitroxide units. For Tb(**3**), the decrease in $\chi_M T$ in 190 – 300 K, and the increase in 18 – 190 K may be the result of a balance among the ferromagnetic Tb(III)-coordinated NO interaction, the antiferromagnetic Rad–Rad interaction, and the other contributions. The observed ferromagnetic interaction is agreement with those reported Tb(III)-radical complexes [21][25][40].

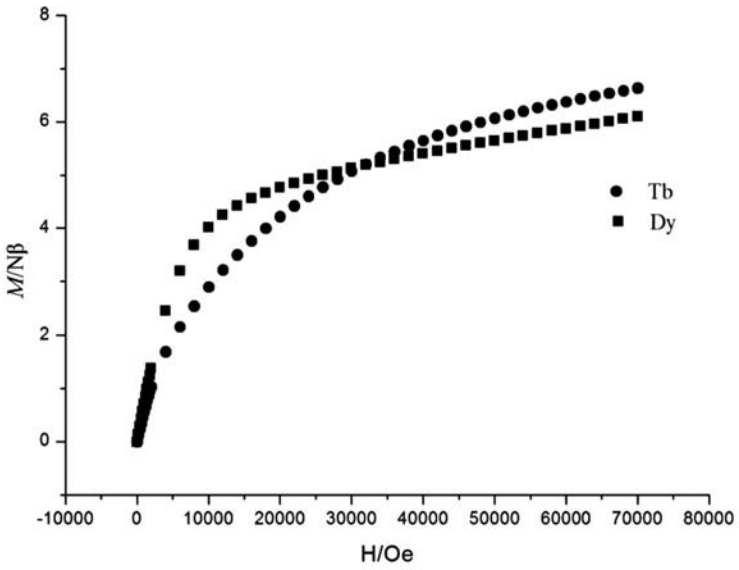

Fig. 8. Field dependence of magnetization for Tb(**3**) and Dy(**4**).

The decrease in $\chi_M T$ value below 18 K may be ascribed to a combination of the intramolecular Rad–Rad antiferromagnetic interaction, intermolecular antiferromagnetic magnetic coupling, and the progressive depopulation of excited *Stark* sublevels. For Dy(**4**), the gradual decrease in $\chi_M T$ value upon cooling is the total result of exchange interactions between the paramagnetic species, the crystal field, and spin–orbit effects. The interaction between Dy(III) and directly coordinated nitroxide group is frequently known to be antiferromagnetic [12][13][44]. The affinity of these magnetic interactions with the electronic configuration of 4f orbitals is apparently based on the systematic investigation of the isostructural series of complexes. Meanwhile, the magnetic interaction is also sensitive to the local crystal field around the Ln(III) center [23][40].

Conclusions

With a new nitronyl nitroxide radical $NITPh(MeO)_2$, we have successfully obtained four similar mononuclear lanthanide-radical complexes $\{Ln(hfac)_3[NITPh(MeO)_2]_2\}$ (Ln = Eu(**1**), Gd(**2**), Tb(**3**), Dy(**4**)). The magnetic studies show that there are antiferromagnetic interactions between Ln(III) and radicals in **1** and **4**, meanwhile ferromagnetic interaction in **3**. For complex **2**, there are weak ferromagnetic interactions between Gd(III) ion and radicals, and antiferromagnetic interaction between two intramolecular radicals.

Tb(III) and Dy(III) are usually selected to construct SMMs or SCMs compounds, due to their large magnetic anisotropy [8]. For the reported SMMs containing lanthanide ions, the slow magnetic relaxation mainly results from single-ion relaxation, which is extremely sensitive to the strength and symmetry of the local crystal field around the lanthanide center [23]. Comparison of the magnetic behaviors of complexes **3** and **4** with those of previously reported Ln(III)-radical SMMs [22][23][25], no SMM behavior is found for **3** and **4**. It indicates that $NITPh(MeO)_2$ is not the suitable ligand for the superparamagnetic systems in this kind of Ln(III)-radical complexes. The substituent -$Ph(MeO)_2$ was firstly utilized to modify the NITR radical. The fact further indicates that the electronic effects of substituents on the ligand can influence the magnetic behavior of the Ln(III) complex greatly.

This project is supported by the *National Natural Science Foundation of China* (No. 21173067) and the *Hebei Natural Science Foundation* (No. B2011205037).

Supplementary Material

Supporting information for this article is available on the WWW under http://dx.doi.org/10.1002/hlca.201600152.

Experimental Part

General

All reagents are of anal. grade and without further purification. The hexafluoroacetylacetonate (hfac) and 3,4-dimethoxybenzaldehyde were purchased from *J&K Chemical Company*. IR Spectra were recorded in the range of 400 – 4000 cm^{-1} on a FT-IR-8900 spectrophotometer with samples as KBr disks; $\tilde{\nu}$ in cm^{-1}. Elemental analyses for C, H, and N were obtained using a *Model 1112 Flash EA* elemental analyzer; in %. Variable temp. magnetic susceptibilities were measured on a *Quantum Design MPMS*, *Squid-VSM* in the range 2 – 300 K in an

Table 1. Crystallographic data and refinement parameters for complexes **1** – **4**

	1	**2**	**3**	**4**
Empirical formula	$C_{45}H_{45}EuF_{18}N_4O_{14}$	$C_{45}H_{45}GdF_{18}N_4O_{14}$	$C_{45}H_{45}TbF_{18}N_4O_{14}$	$C_{45}H_{45}DyF_{18}N_4O_{14}$
Formula weight	1359.81	1365.10	1366.77	1370.35
Temperature [K]	298(2)	298(2)	298(2)	293(2)
Crystal system	Monoclinic	Monoclinic	Monoclinic	Monoclinic
Space group	C2/*c*	C2/*c*	C2/*c*	C2/*c*
a [Å]	20.9969(18)	20.9933(18)	20.9934(17)	20.9738(19)
b [Å]	11.7280(9)	11.7221(9)	11.6859(9)	11.7189(9)
c [Å]	23.296(2)	23.257(2)	23.262(2)	23.298(2)
β [°]	91.185(2)	91.162(2)	91.295(2)	91.371(2)
V [Å^3]	5735.5(8)	5721.9(8)	5705.3(8)	5724.8(8)
Z	4	4	4	4
$D_{calcd.}$ [g cm^3]	1.575	1.585	1.591	1.590
μ [mm^{-1}]	1.241	1.280	1.361	1.426
F(000)	2720	2724	2728	2732
θ Range for data collection [°]	2.59 – 25.02	2.64 – 25.02	2.64 – 25.02	2.67 – 25.02
Limiting indices	$-24 \le h \le 24$	$-24 \le h \le 21$	$-24 \le h \le 24$	$-24 \le h \le 24$
	$-13 \le k \le 13$	$-11 \le k \le 13$	$-13 \le k \le 13$	$-13 \le k \le 13$
	$-20 \le l \le 27$	$-26 \le l \le 27$	$-27 \le l \le 27$	$-27 \le l \le 25$
Reflections collected/unique	14080/5044	14049/5027	23356/5028	11317/4590
	[R_{int} = 0.0463]	[R_{int} = 0.0358]	[R_{int} = 0.1064]	[R_{int} = 0.0914]
Goodness-of-fit on F^2	1.024	1.051	1.054	1.014
R_1 [$I > 2\sigma(I)$]	0.0334, 0.0425	0.0309, 0.0404	0.0504, 0.0694	0.0585, 0.0781
wR_2 (all data)	0.0751, 0.0791	0.0670, 0.0707	0.0979, 0.1081	0.1133, 0.1264

external magnetic field of 1 kOe, and the diamagnetism corrections were corrected with the *Pascal* constants. Alternating-current (ac) susceptibilities were performed under 2000 DC field and 3.5 Oe AC field with different oscillating frequency.

Ln(hfac)$_3$·2 H$_2$O (Ln(III) = Eu(**1**), Gd(**2**), Tb(**3**), Dy(**4**)). They were prepared according to the literature method [45].

Radical NITPh(MeO)$_2$

It was prepared by condensation of 2,3-bis(hydroxyamino)-2,3-dimethylbutane with 3,4-dimethoxybenzaldehyde, followed by oxidation with $NaIO_4$ according the literature [46]. It was purified by column chromatography on neutral Al_2O_3 (petroleum ether/CH_2Cl_2 3:1 as eluent). The radical NITPh(MeO)$_2$ crystallized from the solvent as dark blue crystal. ESR and XRD spectra of NITPh(MeO)$_2$ can be seen in SI (Fig. S11 and S12).

Syntheses of Complexes **1** – **4**

All of them were synthesized by dissolving Ln(hfac)$_3$ · 2 H$_2$O (0.03 mmol) (Ln = Eu(**1**), Gd(**2**), Tb(**3**), Dy(**4**)) in dry heptane (20 ml). After heating to reflux for 1 h, the soln. was cooled to 65 °C, to which a soln. of NITPh(MeO)$_2$ (0.06 mmol) in CH_2Cl_2 (4 ml) was added. The resulting soln. was stirred with refluxing for 30 min, and then cooled and filtered at r.t. The filtrates were allowed to stand at r.t. for slow evaporation. After *ca.* 5 d, deep blue crystals were obtained.

Eu(hfac)$_3$[NITPh(MeO)$_2$]$_2$ (**1**). Yield: 0.019 g (46%). IR: 1658*vs*, 1529*s*, 1508*s*, 1400*s*, 1256*vs*, 1203*s*, 1145*s*, 1022*w*. Anal. calc. for $C_{45}H_{45}F_{18}EuN_4O_{14}$ (1359.79): C 39.75, H 3.34, N 4.12; found: C 39.25, H 3.45, N 4.34.

Gd(hfac)$_3$[NITPh(MeO)$_2$]$_2$ (**2**). Yield: 0.017 g (42%). IR: 1659*vs*, 1529*s*, 1508*s*, 1400*s*, 1255*vs*, 1201*s*, 1146*s*, 1022*w*. Anal. calc. for $C_{45}H_{45}F_{18}GdN_4O_{14}$ (1365.08): C 39.59, H 3.32, N 4.10; found: C 39.25, H 3.21, N 4.23.

Tb(hfac)$_3$[NITPh(MeO)$_2$]$_2$ (**3**). Yield: 0.018 g (43%). IR: 1655*vs*, 1529*s*, 1508*s*, 1400*s*, 1256*vs*, 1200*s*, 1146*s*, 1024*w*. Anal. calc. for $C_{45}H_{45}F_{18}TbN_4O_{14}$ (1366.75): C 39.54, H 3.32, N 4.10; found: C 39.19, H 3.19, N 4.25.

Dy(hfac)$_3$[NITPh(MeO)$_2$]$_2$ (**4**). Yield: 0.019 g (47%). IR: 1659*vs*, 1530*s*, 1508*s*, 1400*s*, 1258*vs*, 1202*s*, 1146*s*, 1024*w*. Anal. calc. for $C_{45}H_{45}F_{18}DyN_4O_{14}$ (1370.33): C 39.44, H 3.31, N 4.10; found: C 39.31, H 3.22, N 4.02.

X-Ray Single-Crystal Analysis of Complexes **1** – **4**[1])

The determination of the unit cell and data collection for the complexes were performed with a graphite-monochromated MoK_α radiation (λ = 0.71073 Å) on a *SMART APEX II CCD* area detector. The φ–ω scan technique was employed. All of the structures were solved primarily by direct methods and refined by full-matrix least squares techniques based on F^2. All non-H-atoms were refined with anisotropic thermal parameters. The H-atoms were set in calculated positions and refined as riding atoms

[1]) CCDC-1419313 (for **1**), 1419314 (for **2**), 1419315 (for **3**) and 1419316 (for **4**) contain the supplementary crystallographic data for complexes **1** – **4**, respectively.

Table 2. Selected bond lengths ([Å]) and bond angles ([°]) for complexes **1** – **4**

1		**2**		**3**		**4**	
Eu(1)–O(2)	2.358(2)	Gd(1)–O(4)	2.344(2)	Tb(1)–O(1)	2.335(3)	Dy(1)–O(6)	2.330(5)
Eu(1)–O(4)	2.360(2)	Gd(1)–O(2)	2.348(2)	Tb(1)–O(6)	2.336(4)	Dy(1)–O(1)	2.333(4)
Eu(1)–O(3)	2.418(2)	Gd(1)–O(3)	2.405(2)	Tb(1)–O(7)	2.390(4)	Dy(1)–O(7)	2.382(4)
Eu(1)–O(1)	2.473(2)	Gd(1)–O(1)	2.424(2)	Tb(1)–O(5)	2.413(4)	Dy(1)–O(5)	2.407(4)
Eu(1)–O(2)[a])	2.358(2)	Gd(1)–O(4)[a])	2.344(2)	Tb(1)–O(1)[a])	2.335(3)	Dy(1)–O(6)[a])	2.330(5)
Eu(1)–O(4)[a])	2.360(2)	Gd(1)–O(2)[a])	2.348(2)	Tb(1)–O(6)[a])	2.336(4)	Dy(1)–O(1)[a])	2.333(4)
Eu(1)–O(3)[a])	2.418(2)	Gd(1)–O(3)[a])	2.405(2)	Tb(1)–O(7)[a])	2.390(4)	Dy(1)–O(7)[a])	2.382(4)
Eu(1)–O(1)[a])	2.473(2)	Gd(1)–O(1)[a])	2.424(2)	Tb(1)–O(5)[a])	2.413(4)	Dy(1)–O(5)[a])	2.407(4)
N(1)–O(4)	1.312(3)	N(1)–O(4)	1.310(3)	N(1)–O(1)	1.310(5)	N(1)–O(1)	1.298(6)
N(2)–O(5)	1.271(4)	N(2)–O(5)	1.273(4)	N(2)–O(2)	1.271(5)	N(2)–O(2)	1.281(7)
N(1)–C(9)	1.328(4)	N(1)–C(9)	1.330(4)	N(1)–C(1)	1.328(6)	N(1)–C(1)	1.321(9)
N(2)–C(9)	1.368(4)	N(2)–C(9)	1.369(4)	N(2)–C(1)	1.372(6)	N(2)–C(1)	1.381(9)
O(4)–Eu(1)–O(4)[a])	143.2(1)	O(4)[a])–Gd(1)–O(4)	143.3(2)	O(1)–Tb(1)–O(1)[a])	142.8(2)	O(1)[a])–Dy(1)–O(1)	142.9(2)

[a]) Symmetry transformations used to generate equivalent atoms: $-x + 1$, y, $-z + 1/2$.

with a common fixed isotropic thermal parameter [47] [48]. Because of the thermal vibration, some restraints were used for solving the disorder of some F-atoms in complexes **1** – **4**. Crystallographic data and details of structural determination refinement for **1** – **4** are summarized in *Table 1*. Their selected bond lengths and angles are listed in *Table 2*. The detailed bond lengths and angles others are placed in the SI (Tables S1 – S4). Powder X-ray diffraction measurements were recorded on a *Bruker D8* X-ray diffractometer using CuK_α radiation, and the XRD spectra of **1** – **4** can be seen in SI (Fig. S4 – S7).

REFERENCES

[1] S. Demir, I. R. Jeon, J. R. Long, T. D. Harris, *Coord. Chem. Rev.* **2015**, *289 – 290*, 149.
[2] D. Luneau, P. Rey, *Coord. Chem. Rev.* **2005**, *249*, 2591.
[3] C. Train, L. Norel, M. Baumgarten, *Coord. Chem. Rev.* **2009**, *253*, 2342.
[4] C. Christian, E. Heintze, B. Lapo, *Dalton Trans.* **2014**, *43*, 4220.
[5] M. N. Leuenberger, D. Loss, *Nature* **2001**, *410*, 789.
[6] L. Bogani, W. Wernsdorfer, *Nat. Mater* **2008**, *7*, 179.
[7] F. Troiani, M. Affronte, *Chem. Soc. Rev.* **2011**, *40*, 3119.
[8] L. Bogani, *J. Appl. Phys.* **2011**, *109*, 07B115.
[9] Y. Zhang, T. Han, X. Q. Liu, A. Yu, P. Cheng, *Inorg. Chem. Commun.* **2015**, *57*, 1.
[10] T. Tsukuda, T. Suzuki, S. Kaizaki, *Polyhedron* **2007**, *26*, 3175.
[11] T. Nakamura, T. Ishida, *Polyhedron* **2015**, *87*, 302.
[12] X. L. Wang, P. P. Xu, X. Bao, F. W. Wang, Y. H. Chen, Y. J. Wei, Z. Anorg, *Allg. Chem.* **2013**, *639*, 176.
[13] M. Y. Song, L. M. Wen, S. P. Wang, S. T. Yang, *Inorg. Chim. Acta* **2015**, *430*, 1.
[14] A. Caneschi, D. Gatteschi, N. Lalioti, *Angew. Chem., Int. Ed.* **2001**, *40*, 1760.
[15] L. Bogani, C. Sangregorio, R. Sessoli, D. Gatteschi, *Angew. Chem., Int. Ed.* **2005**, *44*, 5817.
[16] K. Bernot, L. Bogani, A. Caneschi, D. Gatteschi, R. Sessoli, *J. Am. Chem. Soc.* **2006**, *128*, 7947.
[17] X. L. Wang, X. Bao, P. P. Xu, L. Li, *Eur. J. Inorg. Chem.* **2011**, 3586.
[18] R. N. Liu, Y. Ma, P. P. Yang, X. Y. Song, G. F. Xu, J. K. Tang, L. C. Li, *Dalton Trans.* **2010**, *39*, 3321.
[19] R. N. Liu, C. X. Xiong, S. P. Zhao, J. Xu, Q. Li, D. Fang, *Inorg. Chem. Commun.* **2012**, *22*, 104.
[20] G. Poneti, K. Bernot, L. Bogani, A. Caneschi, R. Sessoli, *Chem. Commun.* **2007**, 1807.
[21] H. X. Tian, R. Liu, X. L. Wang, P. P. Yang, Z. X. Li, L. C. Li, D. Z. Liao, *Eur. J. Inorg. Chem.* **2009**, 4498.
[22] J. X. Xu, Y. Ma, D. Z. Liao, G. F. Xu, J. K. Tang, C. Wang, N. Zhou, *Inorg. Chem.* **2009**, *48*, 8890.
[23] X. L. Mei, R. N. Liu, C. Wang, P. P. Yang, L. C. Li, D. Z. Liao, *Dalton Trans.* **2012**, *41*, 2904.
[24] R. Murakami, T. Ishida, S. Yoshii, H. Nojiri, *Dalton Trans.* **2013**, *42*, 13968.
[25] N. Zhou, Y. Ma, C. Wang, G. F. Xu, J. K. Tang, J. X. Xu, S. P. Yan, P. Cheng, *Dalton Trans.* **2009**, 8489.
[26] X. L. Wang, L. C. Li, D. Z. Liao, *Inorg. Chem.* **2010**, *49*, 4735.
[27] K. Bernot, F. Pointillart, P. Rosa, M. Etienne, R. Sessoli, D. Gatteschi, *Chem. Commun.* **2010**, *46*, 6458.
[28] X. L. Wang, H. X. Tian, Y. Ma, P. P. Yang, L. C. Li, D. Z. Liao, *Inorg. Chem. Commun.* **2011**, *14*, 1728.
[29] E. Coronado, C. Giménez-Saiz, A. Recuenco, *Inorg. Chem.* **2011**, *50*, 7370.
[30] R. N. Liu, C. M. Zhang, L. C. Li, D. Z. Liao, J. P. Sutter, *Dalton Trans.* **2012**, *41*, 12139.
[31] J. J. Wang, M. Zhu, C. Li, J. Q. Zhang, L. C. Li, *Eur. J. Inorg. Chem.* **2015**, 1368.
[32] R. Liu, L. C. Li, X. L. Wang, P. P. Yang, D. Z. Liao, J. P. Sutter, *Chem. Commun.* **2010**, *46*, 2566.
[33] X. F. Wang, P. Hu, Y. G. Li, L. C. Li, *Chem. Asian J.* **2015**, *10*, 325.
[34] P. Hu, X. F. Wang, Y. Ma, Q. L. Wang, L. C. Li, D. Z. Liao, *Dalton Trans.* **2014**, *43*, 2234.
[35] X. F. Wang, Y. G. Li, P. Hu, J. J. Wang, L. C. Li, *Dalton Trans.* **2015**, *44*, 4560.
[36] E. L. Muetterties, L. J. Guggenberger, *J. Am. Chem. Soc.* **1974**, *96*, 1748.
[37] Y. L. Wang, Y. Y. Gao, Y. Ma, Q. L. Wang, L. C. Li, D. Z. Liao, *CrystEngComm.* **2012**, *14*, 4706.
[38] C. Wang, Y. L. Wang, Y. Ma, Q. L. Wang, L. C. Li, D. Z. Liao, *J. Coord. Chem.* **2012**, *65*, 2830.
[39] Y. H. Wan, L. P. Zhang, L. P. Jin, S. Gao, S. Z. Lu, *Inorg. Chem.* **2003**, *42*, 4985.
[40] M. L. Kahn, J. P. Sutter, S. Golhen, P. Guionneau, L. Ouahab, O. Kahn, D. Chasseau, *J. Am. Chem. Soc.* **2000**, *122*, 3413.
[41] Y. L. Wang, Y. Y. Gao, Y. Ma, Q. L. Wang, L. C. Li, D. Z. Liao, *J. Solid State Chem.* **2013**, *202*, 276.

[42] T. Tsukuda, T. Suzuki, S. Kaizaki, *Inorg. Chim. Acta* **2005**, *358*, 1253.
[43] S. Y. Zhou, X. Li, T. Li, L. Tian, Z. Y. Liu, X. G. Wang, *RSC Advances* **2015**, *5*, 17131.
[44] C. Wang, Y. L. Wang, Z. X. Qin, Y. Ma, Q. L. Wang, L. C. Li, D. Z. Liao, *Inorg. Chem. Commun.* **2012**, *20*, 112.
[45] M. F. Richardson, W. F. Wagner, D. E. Sands, *J. Inorg. Nucl. Chem.* **1968**, *30*, 1275.
[46] E. F. Ullman, J. H. Osiecki, D. G. B. Boocock, R. Darcy, *J. Am. Chem. Soc.* **1972**, *94*, 7049.
[47] G. M. Sheldrick, SHELXS-97, Program for the Solution of Crystal Structure, University of Göttingen, Germany, 1997.
[48] G. M. Sheldrick, SHELXL-97, Program for the Crystal Structure Refinement, University of Göttingen, Germany, 1997.

Received May 27, 2016
Accepted August 8, 2016

